RSC Advances

PAPER

View Article Online
View Journal | View Issue

Cite this: *RSC Adv.*, 2020, **10**, 3756

The effects of different inorganic salts on the structure and properties of ionic liquid plasticized starch/poly(butylene succinate) blends

Zhixin Zhao,[ab] Bei Lei,[ab] Wenhao Du,[ab] Zhaojie Yang,[ab] Danyang Tao,[ab] Yuanfang Tian,[ab] Jin Xu[ab] and Xi Zhang *[ab]

Received 9th October 2019
Accepted 11th January 2020

DOI: 10.1039/c9ra08218b

rsc.li/rsc-advances

1-Butyl-3-methylimidazole chloride ([BMIM]Cl) plasticized starch/poly(butylene succinate) (PBS) blends containing inorganic salts with different cations were prepared by a Haake mixer. The compatibility, thermal behaviors including crystallinity, crystallization temperature and melting temperature, thermal stability, and mechanical properties of these blends were systematically investigated by Fourier transform infrared spectroscopy (FT-IR), scanning electron microscopy (SEM), thermogravimetric analysis (TGA), differential scanning calorimetry (DSC) and X-ray diffraction (XRD). The results showed that the inorganic salts could interact strongly with [BMIM]Cl plasticized starch/PBS blends to improve their mechanical properties, while the thermal stability of the [BMIM]Cl plasticized starch/PBS blends was simultaneously reduced. The SEM results suggested that the compatibility of [BMIM]Cl plasticized starch and PBS was significantly improved with increasing inorganic salt content. Furthermore, by incorporating inorganic salts, the melting enthalpy (ΔH_m), crystallinity (X_c), and cold crystallization temperature (T_{cc}) of the blends were decreased.

Introduction

Due to the continuous consumption of petroleum resources as raw materials for the preparation of polymer materials and the increasing emphasis on environmental pollution caused by the difficult degradation of waste polymer materials, the development of eco-friendly and biodegradable polymers based on natural and non-petroleum resources has been greatly considered by governments and scientific research institutions all over the world.[1–3] In this direction, starch is one of the most promising candidates for environment-friendly blend development. Unlike petroleum-based plastics, starch is one of the most abundant polymeric materials derived from renewable resources.[4] It is a fully biodegradable and annually renewable inexpensive polymer.[5,6] However, since the intra- and intermolecular hydrogen bonds are very strong,[7] the thermal decomposition temperature of starch is lower than its melting point, which results in the poor processability of starch. Plasticization of starch must be carried out using low molecular weight compounds such as glycerol to form thermoplastic starch (TSP) for processing on conventional processing equipment, which would further reduce the mechanical strength of the resulting materials.[8,9] These are the key issues that need to be solved, before these attractive materials can find meaningful applications in various products.

Previous studies have found that blending with aliphatic polyesters is an effective way to solve these problems and broaden the application of starch.[10–12] As one of the most commonly used aliphatic polyesters, poly(butylene succinate) (PBS) is a biodegradable thermoplastic polymer that can be obtained by fermentation of biological resources, which has good processability, thermal stability, excellent mechanical properties, good water resistance, and dimensional stability.[13–15] Therefore, starch and PBS are mixed, and it is expected to produce eco-friendly materials with low cost and good performance. Nevertheless, PBS behaves hydrophobicity because of the repeated aliphatic units on the backbone, and starch exhibits hydrophilicity with strong intra- and intermolecular hydrogen bonds, which result in poor adhesion between the two components and hence poor performance. Obviously, simply blending starch with PBS does not result in the ideal blend materials.[12,16]

When attempting to improve the mechanical properties of starch/PBS blend, two general methods were taken: (a) using compatibilizers between PBS and the starch granules; and (b) plasticizing the starch granules to make them easier dispersed into PBS matrix. As a general way of the method (b), starch plasticizers, such as glycerol, urea, water and citric acid, were used to break the crystallinity and the strong hydrogen bond within the starch granules. However, the use of these

[a]State Key Laboratory of Polymer Materials Engineering, Sichuan University, Chengdu 610065, People's Republic of China. E-mail: zhangxi6352@163.com; Tel: +8613808072562

[b]Polymer Research Institute, Sichuan University, Chengdu 610065, People's Republic of China

plasticizers still has some disadvantages such as water sensitivity, phase separation, and retrogradation, which may result in brittleness and hence limit the applications.[17]

Recently, ionic liquids have drawn much attention due to the significant capacity in plasticizing starch compared with the conventional plasticizers. Ionic liquid (IL) is a type of organic salts with melting point below 100 °C, which were found to be more efficient to depress the glass transition temperature and reduce the water sensitivity of TSP. Based on the study conducted by Sankri *et al.*,[18] the mechanism of [BMIM]Cl plasticizing starch is considered to be that each ion pair Cl^-/$[BMIM]^+$ forms complex with one C–O–H group of starch. Consequently, strong hydrogen bonds are formed between the anions of IL and the –OH groups of starch. The intra- and inter-molecular hydrogen bonds of starch chains are destroyed, leading to the sufficient plasticization for starch. However, previous studies have found a problem that the strength of the starch/PBS blends is greatly reduced after plasticized by IL.

The aim of this work is to innovate the modified method of starch/PBS, further optimizing the strength of the IL plasticized starch/PBS blends. Fig. 1 reveals the mechanism that, we chose inorganic salts of magnesium chloride and lithium chloride as co-plasticizers because the metallic ions in inorganic salts can interact with the oxygen atoms in starch and PBS. This interaction can alter the aggregation structure of the starch/PBS blends, adjust the binding strength of the "IL-macromolecule" in the starch/PBS blend, and inhibit the decrease in strength due to the introduction of [BMIM]Cl, thereby provide a new idea for the modification of the starch/PBS blends.

Experimental

Materials

Poly(butylene succinate) was kindly provided by Anqing Hexing Chemical Co., Ltd. (Anqing, P. R. China). Corn starch was purchased from Xiadian Corn Development Industrial Co., Ltd. (Xi'an, P. R. China), which was edible level. 1-Butyl-3-methylimidazolium chloride ([BMIM]Cl) (97% purity) was obtained from Aladdin Biochemical Technology Co., Ltd. (Shanghai, P. R. China), which was used without any further purification. Magnesium chloride ($MgCl_2$) and lithium chloride (LiCl) were purchased from Kelong Chemical Co. (Chengdu, P. R. China), which was analytical purity.

Sample preparation

Samples were prepared by the melt blending method. First, starch and PBS were dried in a vacuum oven (p < 0.3 MPa) at 105 °C for 5 h. Starch and plasticizers ([BMIM]Cl and inorganic salts) were pre-mixed at room temperature for 2 h, and then placed in a vacuum oven at 60 °C for 72 h before blending. The mixture was further plasticized in HAAKE Rheomix OS Torque Rheometer at 125 °C with a rotor speed of 70 rpm for 15 min. The obtained thermoplastic starch samples were designated TSP (plasticized by IL), TSPM (plasticized by IL and $MgCl_2$) or TSPL (plasticized by IL and LiCl), respectively.

The starch/PBS blends were then prepared by melting TSP (or TSPM, TSPL) and PBS in HAAKE Mixer at 125 °C with a rotor speed of 70 rpm for 15 min. The formulations of samples were listed in Tables 1 and 2. Finally, the blends were processed with a micro-injection molding machine (HAAKE MINIJET PRO) to obtain specimens for mechanical and other measurements. The barrel and mold temperatures during micro-injection molding were 125 and 25 °C, respectively. The micro-injection and packing pressure were both 400 bar. Dumb-bell specimens (width 4 mm, thickness 2 mm, length of parallel part 30 mm, and total length 75 mm) were prepared for the tensile test.

Characterizations

Fourier transform infrared (FT-IR) spectroscopy. The samples were dried in a vacuum oven at 105 °C for 5 h to remove water and then crushed into powder with a pulverizer. The infrared spectra were measured using a Fourier transform infrared spectrophotometer (Nicolet 560) with a spectral resolution of 4 cm^{-1} and the scanning range of 400 to 4000 cm^{-1}.

Scanning electron microscopy (SEM). The dumb-bell specimens were frozen by liquid nitrogen for 1 hour before brittle fracture. The morphology of the samples was examined under a scanning electron microscope JSM-5900LV (JEOL, Japan). The

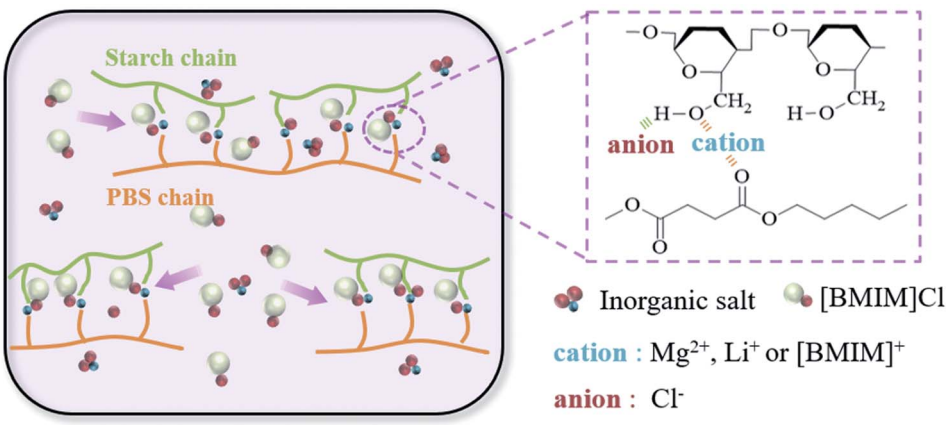

Fig. 1 The mechanism of TSP blends modified with different inorganic salts.

Table 1 Mixing formulations of starch/PBS blends plasticized by IL and $MgCl_2$

Samples	Starch/(wt%)	PBS/(wt%)	IL/starch ratio/(wt/wt)	$MgCl_2$/starch ratio/(wt/wt)
TSP	40	60	0.25	0
TSPM1	40	60	0.25	0.025
TSPM2	40	60	0.25	0.05
TSPM3	40	60	0.25	0.075
TSPM4	40	60	0.25	0.1

surfaces were coated with platinum prior to examination. The accelerating voltage was 10 kV.

Thermal gravity analysis (TGA). TGA was performed by TA2950 TGA thermal analysis instrument (Du Pont, UK). The samples for testing were heated from room temperature to 600 °C at a heating rate of 10 °C min^{-1}.

Differential scanning calorimetry (DSC). The DSC measurements were performed by a differential scanning calorimeter (PerkinElmer DSC8500, São Paulo, Brazil). Samples (3–5 mg) were placed in sealed aluminum crucibles under a flow of nitrogen for the DSC tests. Each sample was first heated from 30 to 140 °C at a rate of 50 °C min^{-1}, kept at 140 °C for 3 min to eliminate thermal history, cooled to 30 °C at a cooling rate of 10 °C min^{-1}, kept at 30 °C for 2 min, and then reheated at a rate of 10 °C min^{-1} to 140 °C.

X-ray diffraction (XRD) measurements. The XRD test was carried out using an X'Pert Pro MPD diffractometer manufactured by Philips Analytical Company of Netherlands, with nickel lter Cu Kα as the radiation source. The acceleration voltage was 50 kV and the current was 35 mA. The samples were continuously scanned over the 2θ range from 5 to 50°.

Mechanical properties test. The mechanical properties (tensile strength (TS), elongation at break (% Eb) and Young's modulus) of the sample was determined using a tensile testing equipment (Instron 5567, Norwood, MA, USA). The crosshead speed was 20 mm min^{-1}. The initial gauge length of the specimen was 20 mm. The width of each tensile sample was 4 mm. The sample thickness was measured with a micrometer in triplicate. All samples were balanced in 30% relative humidity (RH) at 25 °C for 48 h prior to test. Five specimens were used for each group, and the average values plus the standard deviation were determined. *t*-Test was carried out to determine the statistically significant difference ($p < 0.05$) among the mechanical properties using STATA (STATA 11.2 for windows).

Results and discussion

FT-IR analysis

The interaction between inorganic salts and TSP is mainly the electronic interaction between the anion and cation of the inorganic salt and the –OH of starch and PBS. The movement of the stretching vibration peak of –OH can reflect the intensity of the electron interaction. Therefore, FT-IR was used to characterize the TSP before and after inorganic salt modification. The conclusion below is only suggested by our test results. Fig. 2 shows the FTIR spectra of TSPM and TSPL modified with $MgCl_2$ or LiCl, together with those of TSP. For TSP, the peak at 3411 cm^{-1} corresponds to the stretching vibration absorption peak of starch and PBS molecular chain,[19] the peak at 1084 cm^{-1} corresponds to the stretching vibration peak of C–O in the C–O–H group on the starch molecule, and the peak at 1028 cm^{-1} corresponds to the stretching vibration peak of C–O in C–O–C on the starch molecular chain, the peak at 1723 cm^{-1} corresponds to the stretching vibration absorption peak of C=O in the ester group on the PBS molecule.[20] For TSPM and TSPL, the FTIR spectra do not show any other absorption peaks of new chemical groups, indicating that neither $MgCl_2$ nor LiCl reacted with TSP. However, inorganic salts could further affect the absorption peaks of hydroxyl and ester groups in TSP. It's worth noting that the –OH and C=O peaks of TSP modified by $MgCl_2$ and LiCl shifted to the direction of high wavenumber. This indicates that inorganic salt has strong interaction with the molecular chains of TSP and PBS. This phenomenon is probably due to the fact that electron-deficient Mg^{2+} or Li^+ forms an electronic interaction with the oxygen atoms in the hydroxyl group on the starch molecule and the ester group on the PBS molecule, while the electron-rich Cl^- interacts with the hydrogen atoms of the hydroxyl group in the starch and PBS molecules. It can be speculated that inorganic salts may weaken

Table 2 Mixing formulations of starch/PBS blends plasticized by IL and LiCl

Samples	Starch/(wt%)	PBS/(wt%)	IL/starch ratio/(wt/wt)	LiCl/starch ratio/(wt/wt)
TSP	40	60	0.25	0
TSPL1	40	60	0.25	0.025
TSPL2	40	60	0.25	0.05
TSPL3	40	60	0.25	0.075
TSPL4	40	60	0.25	0.1

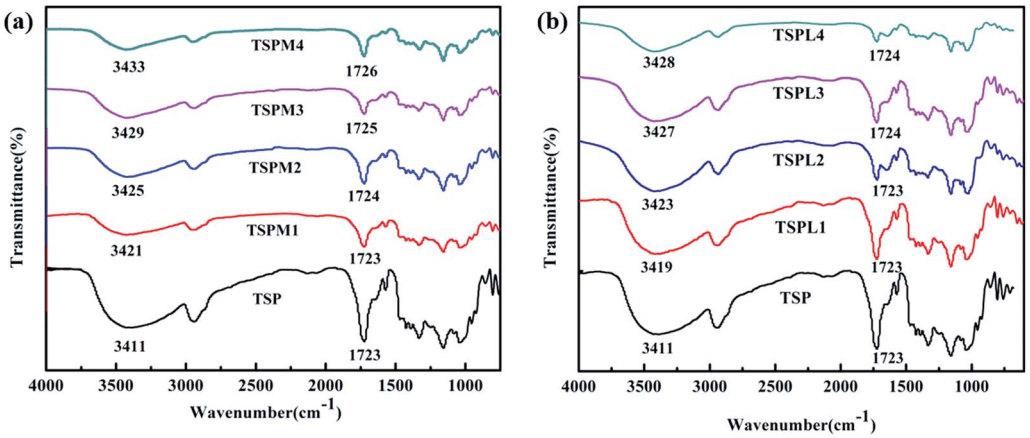

Fig. 2 The FTIR spectra of TSP blends modified with $MgCl_2$ (a) and LiCl (b).

the hydrogen bonds and lead to the change of aggregation structure and properties of TSP.

Furthermore, the comparison between TSPM and TSPL shows that the effect of $MgCl_2$ on the red shift of the hydroxyl and ester peaks in starch and PBS is more obvious than that of LiCl, when the contents of the two inorganic salts are the same. This may be due to that when the anion type is the same, the ion radius of Li^+ is larger than Mg^{2+}, resulting in a relatively weaker ability to enter the molecular chain of starch and PBS, thus the interaction of Li^+ with the hydroxyl and ester groups on TSP is weaker than that of Mg^{2+}. That is, the smaller the ionic radius of the cation in inorganic salt, the stronger the interaction of the ions with the hydroxyl and ester groups, and the more obvious the red shift of the absorption peak of the hydroxyl and ester groups.

Scanning electron microscopy

The performance and properties of blending materials not only depend on the properties of the individual components but also on their interfacial compatibility, so increasing the compatibility between the components is essential for improving the performance of the materials.

In order to investigate the effect of inorganic salts on the compatibility of TSP blends, the fractured surfaces of TSP, TSPM, and TSPL were observed by SEM. As shown in Fig. 3a, the TSP blends still had an obvious two-phase structure, in which the starch granules plasticized with IL were embedded in the continuous phase of the PBS matrix then formed the sea-island structure, with some starch granules falling off the cross section and forming grooves. Obviously, the interface strength between the two-phase adhesion was very weak, and the TSP blend was very brittle. This might be because the starch granules plasticized with IL were not completely broken into the PBS phase during the dissolution process. Some starch granules were retained and had low compatibility with PBS, eventually resulting in a clear phase separation structure. In contrast, the granular structure was partially absent from TSPM1 (Fig. 3b), TSPL1 (Fig. 3d), and TSPL4 (Fig. 3e), but almost totally disappeared from TSPM4 (Fig. 3c), which indicated that the adhesion of the two phases was significantly enhanced by the introduction of inorganic salts. This might be due to that inorganic salts interfered with the formation of intramolecular hydrogen bonds within the starch and PBS itself, thereby destroying the crystalline structure of starch and PBS. It can be speculated that inorganic salt plays a certain role in promoting starch/PBS blending.

Furthermore, comparing TSPL4 and TSPM4, it was found that there were still some residual starch granules and cracks in the fracture surface of the TSPL4 blend, while the surface of the TSPM4 blend was continuous, homogeneous, and smooth, indicating that the starch could be uniformly dispersed in the PBS matrix. By combining the results of FT-IR spectra, this phenomenon might be due to the fact that the high-valent Mg^{2+} has better electron defect ability than Li^+, generate stronger electronic interaction with the hydroxyl group in the starch molecular chain and the ester group in the PBS molecular chain. As a result, the inter- and intra-molecular hydrogen bonds of starch and PBS were destroyed, thereby effectively improving the compatibility of starch and PBS in TSPM blends (our conclusion is only suggested by our results).

Thermal stability analysis

Processability and applicability of polymer systems depends greatly on their thermal stability. The effect of inorganic salts on the thermal stability of TSP blends were consequently studied by TGA. Fig. 4 shows the TGA curves of TSP blends modified with inorganic salts containing different cations, and the corresponding initial thermal decomposition temperatures (T_i) were recorded in Tables 3 and 4. The TSP blend mainly undergo three-stage thermal degradation. The first step corresponds to the volatilization of water. The second step is related to the pyrolysis of starch, and the third stage with a maximum decomposition temperature of more than 340 °C is the thermal degradation of PBS chains. It can be seen that with the addition of $MgCl_2$ and LiCl (from 0 to 4 wt%), the initial thermal decomposition temperatures of the TSPM and TSPL decreased from 243.3 °C to 202.7 °C and 205.1 °C, respectively, indicating the thermal stability of the TSP blends decreased by the

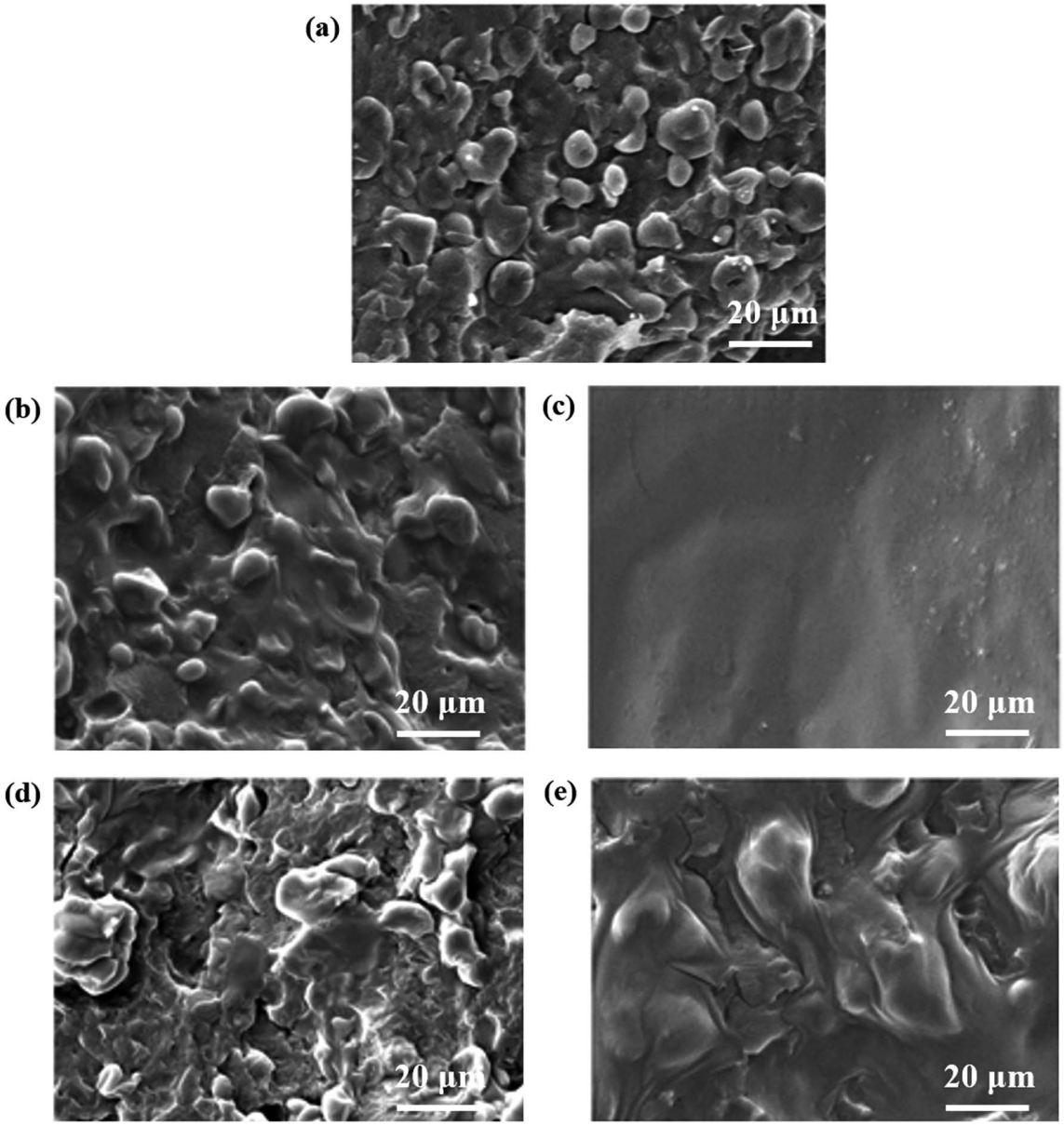

Fig. 3 The SEM micrographs of TSP (a), TSPM1 (b), TSPM4 (c), TSPL1 (d), TSPL4 (e).

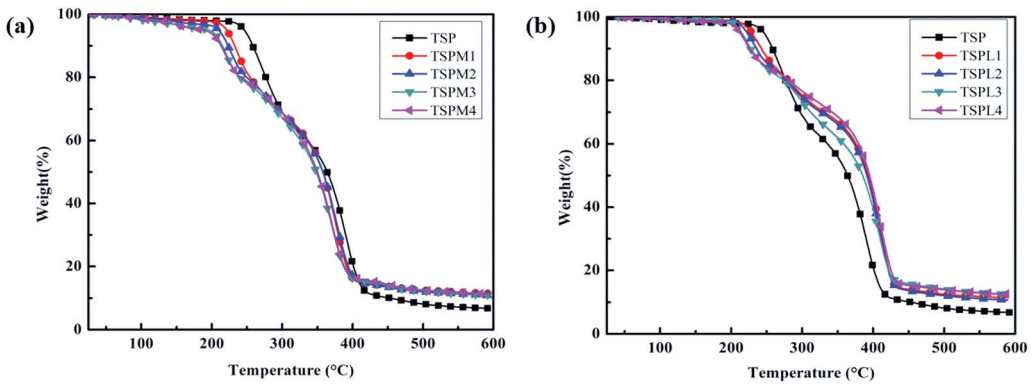

Fig. 4 The TGA curves of TSP blends modified with $MgCl_2$ (a) and LiCl (b).

Table 3 The thermal stability parameters of TSP blends modified with $MgCl_2$

Sample	T_i (°C)	Residue at 600 °C (%)
TSP	243.3	6.78
TSPM1	217.9	11.44
TSPM2	213.5	10.73
TSPM3	204.4	12.48
TSPM4	202.7	12.55

Table 4 The thermal stability parameters of TSP blends modified with LiCl

Sample	T_i (°C)	Residue at 600 °C (%)
TSP	243.3	6.78
TSPL1	220.0	11.47
TSPL2	216.1	10.94
TSPL3	207.2	10.97
TSPL4	205.1	11.27

Table 5 The mass fraction of PBS in all blending materials

Samples	Starch/g	PBS/g	[BMIM]Cl/g	$MgCl_2$/g	α/%
TSP	16	24	4	0	54.55
TSPM1	16	24	4	0.4	54.05
TSPM2	16	24	4	0.8	53.57
TSPM3	16	24	4	1.2	53.10
TSPM4	16	24	4	1.6	52.63
TSPL1	16	24	4	0.4	54.05
TSPL2	16	24	4	0.8	53.57
TSPL3	16	24	4	1.2	53.10
TSPL4	16	24	4	1.6	52.63

Table 6 The DSC data of TSP blends modified with $MgCl_2$

Sample	ΔH_m (J g^{-1})	X_c (%)	T_c (°C)	T_m (°C)	T_{cc} (°C)
TSP	28.63	47.59	64.22	105.89	88.33
TSPM1	25.07	42.05	62.18	106.78	89.01
TSPM2	24.43	41.34	61.40	107.53	89.68
TSPM3	23.03	39.32	60.36	108.61	90.13
TSPM4	21.97	37.84	59.19	109.32	91.71

addition of inorganic salts. This is because the addition of inorganic salt ions further destroys the crystal structure of the TSP blend, resulting in an increase in the amorphous region of the TSP blends, while the molecular chains in the amorphous region are more susceptible to thermal decomposition. Further, $MgCl_2$ and LiCl are Lewis acid salts. Electron-deficient metal

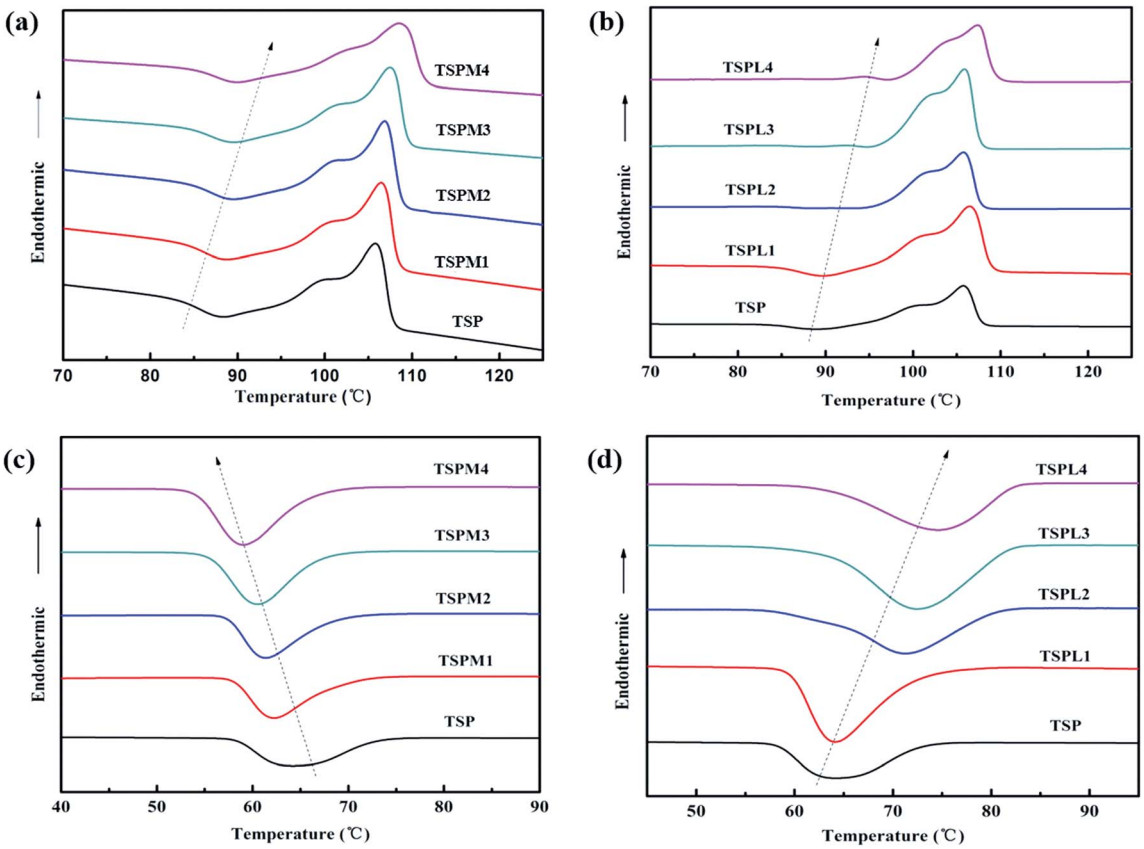

Fig. 5 The DSC melting curves of TSP blends modified with $MgCl_2$ (a) and LiCl (b); the DSC crystallization curves of TSP blends modified with $MgCl_2$ (c) and LiCl (d).

Table 7 The DSC data of TSP blends modified with LiCl

Sample	ΔH_m (J g^{-1})	X_c (%)	T_c (°C)	T_m (°C)	T_{cc} (°C)
TSP	28.63	47.59	64.22	105.89	88.33
TSPL1	25.33	42.48	64.36	106.15	89.90
TSPL2	24.65	40.89	71.31	106.27	94.11
TSPL3	23.72	40.50	72.41	106.96	95.23
TSPL4	22.47	38.71	74.55	107.63	97.44

Table 8 The mechanical properties of TSP blends modified with $MgCl_2$ or LiCl

Sample	Tensile strength (MPa)	Elongation at break (%)
TSP	10.79 ± 0.22	14.06 ± 0.25
TSPMS1	13.34 ± 0.29	15.90 ± 0.31
TSPMS2	14.05 ± 0.32	17.70 ± 0.42
TSPMS3	15.17 ± 0.30	18.36 ± 0.38
TSPMS4	15.80 ± 0.22	19.47 ± 0.33
TSPL1	11.26 ± 0.26	14.23 ± 0.36
TSPL2	12.32 ± 0.22	14.68 ± 0.29
TSPL3	13.47 ± 0.31	14.79 ± 0.21
TSPL4	14.97 ± 0.21	16.37 ± 0.30

cations have stronger effect on accelerating the thermal decomposition process of PBS than that of the crystalline structure as previously reported.[21]

In addition, the comparison between TSPM and TSPL showed that the effect of $MgCl_2$ on T_i was more obvious than that of LiCl, when the contents of the two inorganic salts were the same. This may be due to that the ion radius of Li^+ is larger than Mg^{2+}, resulting in a relatively weaker ability to enter the molecular chain of starch and PBS, thus the obstruction of Li^+ on polymer crystallization is weaker than that of Mg^{2+}. This is consistent with the FTIR and SEM analysis results.

Thermal properties

DSC was used to study the difference in thermal properties between TSP, TSPM and TSPL blends. Fig. 5 shows the DSC thermograms of the first cooling and the second heating processes of these materials. The corresponding thermal data were summarized in Tables 6 and 7. From the melting curves of Fig. 5(a) and (b), the TSP blends modified with $MgCl_2$ and LiCl exhibited a melting bimodal, and there was also an exothermic cold crystallization peak during this process. This phenomenon can be explained by the mechanism of melting-recrystallization.[22–24] Meanwhile, the crystallinity (X_c) of TSP blends modified with inorganic salts is calculated by formula (1):

$$X_c\% = 100\% \times \frac{\Delta H_m}{\Delta H_m^0 \times \alpha} \quad (1)$$

where ΔH_m is the melting enthalpy of different TSP blends, ΔH_m^0 is the melting enthalpy of fully crystallized PBS, which is taken as 110.3 J g^{-1} α is the mass fraction of PBS in all blending materials and is listed in Table 5, respectively.

As shown in Fig. 5(a) and (c) and Table 6, as the $MgCl_2$ content increased, the melting enthalpy (ΔH_m), crystallinity (X_c) and crystallization temperature (T_c) of TSPM decreased, but the cold crystallization temperature (T_{cc}) increased. This is because on the one hand, the electron-deficient Mg^{2+} interacts with the electron-donating oxygen atoms in –OH of starch and ester of PBS, so that the intermolecular force increases, and the energy required for rearrangement of the chains increases, resulting in the increase of the cold crystallization temperature (T_{cc}). On the other hand, the addition of $MgCl_2$ enhances the interaction between starch and PBS, decrease the chain mobility of PBS through the plasticization effect so as to hinder the orderly arrangement of the PBS crystal regions. Therefore, the melting enthalpy (ΔH_m), crystallinity (X_c) and crystallization temperature (T_c) were decreased.

In contrast, for TSPL, with the increase of LiCl content, the melting enthalpy and crystallinity decreased, while the cold crystallization temperature and crystallization temperature increased (Fig. 5(b) and (d) and Table 7). It is worth noting that $MgCl_2$ and LiCl had similar effects on the melting enthalpy, crystallinity and cold crystallization temperature of TSP. However, $MgCl_2$ had a greater influence on the crystallinity of TSP, from 47.59% to 37.84%. This indicated that Mg^{2+} with stronger electron deficient ability and smaller ion radius had

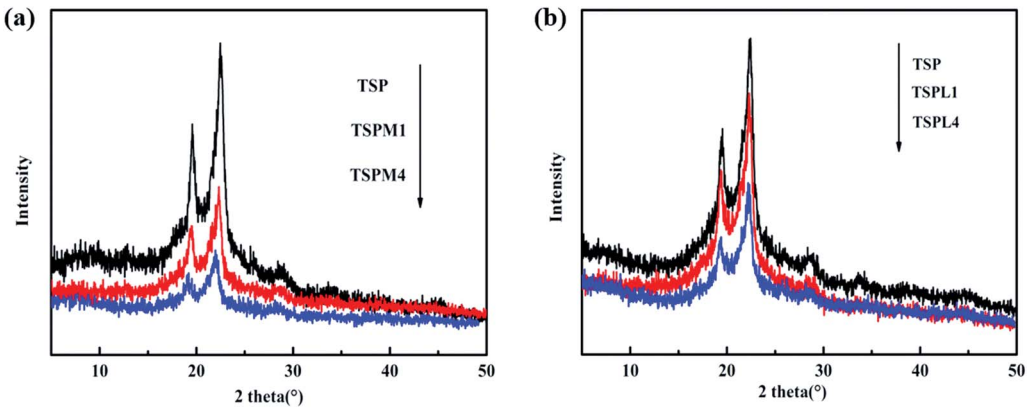

Fig. 6 The XRD diffractograms of TSP blends modified with $MgCl_2$ (a) or LiCl (b).

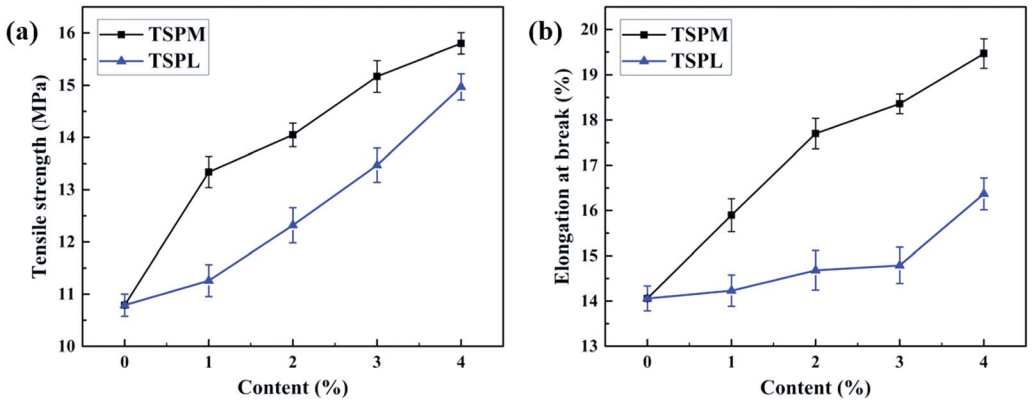

Fig. 7 (a) The tensile strength of TSP blends modified with $MgCl_2$ or LiCl; (b) the elongation at break of TSP blends modified with $MgCl_2$ or LiCl.

stronger interaction with TSP than Li^+, which could more effectively disrupt the crystalline structure of starch and PBS. However, the trend of the crystallization temperature of TSPL is opposite to that of TSPM. It was speculated that in the TSPL system, Li^+ enhanced intermolecular interaction was dominant, which was stronger than the crystallization damage. On the contrary, in the TSPM system, $MgCl_2$ dominated the destruction of crystallization. This could also be confirmed by the following phenomenon: the increase of cold crystallization temperature (T_c) of TSPL system was higher than that of TSPM system, from 88.33 °C to 97.44 °C (T_c of the TSPM system was 91.71 °C).

Crystalline properties

The previous studies have proved that inorganic salts could play the role of plasticizer by destroying the crystal structure of starch/PBS blends.[25] Among them, both the anions and cations in inorganic salts could form the strong coordination effect with –OH, thereby interrupting the inter- and intramolecular hydrogen bonds of starch and PBS, and destroying their crystals. In order to verify this, the effect of inorganic salts on the crystalline property of TSP was studied by XRD (Fig. 6). For TSP, TSPM and TSPL, the three diffraction peaks at 19.5°, 21.5° and 22.5°, corresponding to the (020), (021) and (110) crystal faces,[26,27] respectively, consistent with the characteristic peaks of α crystal of PBS. The diffraction peak positions of the TSP blends do not move or change with the introduction of $MgCl_2$ or LiCl, nor do the new crystal diffraction peaks appear, indicating that the crystalline form of PBS was not modified by starch, IL or inorganic salts.

Moreover, the crystallization peaks intensity of the TSP blends decreased sharply after the addition of inorganic salts, suggesting that most of the starch/PBS crystals were transformed to amorphous phases and $MgCl_2$ or LiCl had a damaging effect on the crystals of TSP blends. The reduction in crystallinity of TSP could be explained by the fact that $MgCl_2$ and LiCl were able to enter the molecular chains of starch and PBS to weaken the inter- and intra-molecular hydrogen bonds of TSP, thus destroy the crystalline structures of TSP. In addition, the intensity of the TSPM crystal peak was weaker than that of the TSPL crystal peak. This is probably because the ionic radius of the magnesium ion is smaller than that of the lithium ion, so magnesium ions can more easily enter into the molecular chains of starch and PBS and destroy their crystallization, which is in good agreement with the FTIR, SEM, TGA and DSC analysis results.

Mechanical properties

The influence of inorganic salts on the mechanical properties of TSP blends was evaluated by tensile testing. According to previous literatures,[28–32] since starch contains a large number of inter- and intra-molecular hydrogen bonds, microcrystals are easily formed, which makes starch and starch-based materials exhibit strong brittleness. As shown in Table 8 and Fig. 7, the tensile strength of TSP was 10.79 MPa and the elongation at break was 14.06%, which also showed obvious brittleness. As expected, the tensile strength and elongation at break of the TSP blends increased significantly after the addition of inorganic salts, while the TSPM blends increased more than the TSPL blends. For TSPM4, the tensile strength increased to 15.80 MPa and the elongation at break increased to 19.47%, which were 46.43% and 38.48% higher than those of the TSP blend, respectively. Meanwhile, for TSPL4, the tensile strength increased to 14.79 MPa and the elongation at break increased to 16.37%, which were 37.07% and 16.43% higher than those of the TSP blend, respectively. This is because the electron-deficient cations of inorganic salts could interact strongly with the oxygen atoms in TSP, enhancing the compatibility of the starch and PBS phases, thereby improving the mechanical strength and flexibility of the blends. In addition, since Mg^{2+} lacked more electrons than Li^+, a stronger electronic interaction could be formed, thus the mechanical properties of TSPM were superior to those of TSPL. From the above results, it was found that the addition of inorganic salts could compensate for the mechanical strength loss of the blend caused by IL, which was expected to provide a new method for controlling the properties of the starch/PBS blends.

Conclusion

In this study, the IL plasticized starch/PBS blends were further modified by magnesium chloride or lithium chloride. FTIR

results showed that electron-deficient Mg^{2+} or Li^{+} could form an electronic interaction with the oxygen atoms in the hydroxyl group on the starch molecule and the ester group on the PBS molecule, while the electron-rich Cl^{-} interacted with the hydrogen atoms of the hydroxyl group in the starch and PBS molecules. Compared with TSP, the addition of inorganic salts could further destroy the ordered arrangement of the molecular chains in the starch and PBS crystal regions, thereby significantly improving the compatibility of starch and PBS. However, thermal stability of TSP blend decreased when magnesium chloride or lithium chloride was incorporated. With the introduction of inorganic salts, the melting enthalpy (ΔH_m), crystallinity (X_c) and cold crystallization temperature (T_{cc}) of TSP were decreased, while the tensile strength and elongation at break were increased. Moreover, compared to LiCl, $MgCl_2$ had a greater influence on those properties of TSP, indicated that Mg^{2+} with stronger electron deficient ability and smaller ion radius had stronger interaction with TSP than Li^{+}, which could more effectively disrupt the crystalline structure of starch and PBS. In summary, the addition of inorganic salts can be used to compensate for the mechanical strength loss caused by [BMIM]Cl modification, which is expected to provide a new idea for the modification of the starch/PBS blends.

Conflicts of interest

The authors declare no conflict of interest.

Acknowledgements

This research was supported by Applied Basic Research Project of Sichuan Province (No. 2017JY0247).

References

1 S. Chen, F.-y. Li, J.-f. Li, X. Sun, J.-f. Cui, C.-w. Zhang, L.-m. Wang, Q. Xie and J. Xu, *RSC Adv.*, 2018, **8**, 12400–12408.
2 S. Lambert and M. Wagner, *Chem. Soc. Rev.*, 2017, **46**, 6855–6871.
3 M. Singhvi and D. Gokhale, *RSC Adv.*, 2013, **3**, 13558–13568.
4 X. Cao, A. Mohamed, S. H. Gordon, J. L. Willett and D. J. Sessa, *Thermochim. Acta*, 2003, **406**, 115–127.
5 V. M. Leloup, P. Colonna and S. G. Ring, *Biotechnol. Bioeng.*, 1991, **38**, 127–134.
6 W. Schulz, H. Sklenar, W. Hinrichs and W. Saenger, *Biopolymers*, 1993, **33**, 363–375.
7 X. F. Ma, J. G. Yu and F. Jin, *Polym. Int.*, 2004, **53**, 1780–1785.
8 A. P. Mathew and A. Dufresne, *Biomacromolecules*, 2002, **3**, 1101–1108.
9 R. C. R. Souza and C. T. Andrade, *Adv. Polym. Technol.*, 2002, **21**, 17–24.
10 L. Chen, X. Qiu, Z. Xie, Z. Hong, J. Sun, X. Chen and X. Jing, *Carbohydr. Polym.*, 2006, **65**, 75–80.
11 R. Mani and M. Bhattacharya, *Eur. Polym. J.*, 2001, **37**, 515–526.
12 J.-B. Zeng, L. Jiao, Y.-D. Li, M. Srinivasan, T. Li and Y.-Z. Wang, *Carbohydr. Polym.*, 2011, **83**, 762–768.
13 J. Xu and B. H. Guo, *Biotechnol. J.*, 2010, **5**, 1149–1163.
14 Z. Zhang, J. Zhang and T. Tian, *RSC Adv.*, 2016, **6**, 73853–73858.
15 M. Zhou, J. Yan, Y. Li, C. Geng, C. He, K. Wang and Q. Fu, *RSC Adv.*, 2013, **3**, 26418–26426.
16 J. W. Li, X. G. Luo, X. Y. Lin and Y. Zhou, *Starch/Staerke*, 2013, **65**, 831–839.
17 A. Bendaoud and Y. Chalamet, *Carbohydr. Polym.*, 2013, **97**, 665–675.
18 A. Sankri, A. Arhaliass, I. Dez, A. C. Gaumont, Y. Grohens, D. Lourdin, I. Pillin, A. Rolland-Sabaté and E. Leroy, *Carbohydr. Polym.*, 2010, **82**, 256–263.
19 A. Sankri, A. Arhaliass, I. Dez, A. C. Gaumont, Y. Grohens, D. Lourdin, I. Pillin, A. Rolland-Sabate and E. Leroy, *Carbohydr. Polym.*, 2010, **82**, 256–263.
20 Y. M. Cai, J. G. Lv and J. M. Feng, *J. Polym. Environ.*, 2013, **21**, 108–114.
21 P. Alexy, D. Kachova, M. Krsiak, D. Bakos and B. Simkova, *Polym. Degrad. Stab.*, 2002, **78**, 413–421.
22 Y. X. Xu, J. Xu, B. H. Guo and X. M. Xie, *J. Polym. Sci., Polym. Phys. Ed.*, 2007, **45**, 420–428.
23 M. Yasuniwa and T. Satou, *J. Polym. Sci., Polym. Phys. Ed.*, 2002, **40**, 2411–2420.
24 S. Zhang, Y. He, Y. Yin and G. Jiang, *Carbohydr. Polym.*, 2019, **206**, 827–836.
25 R. Zullo and S. Iannace, *Carbohydr. Polym.*, 2009, **77**, 376–383.
26 G. Liu, L. Zheng, X. Zhang, C. Li, S. Jiang and D. Wang, *Macromolecules*, 2012, **45**, 5487–5493.
27 J.-B. Zeng, Y.-D. Li, Q.-Y. Zhu, K.-K. Yang, X.-L. Wang and Y.-Z. Wang, *Polymer*, 2009, **50**, 1178–1186.
28 N. Follain, C. Joly, P. Dole and C. Bliard, *J. Appl. Polym. Sci.*, 2005, **97**, 1783–1794.
29 A. Imberty, H. Chanzy, S. Perez, A. Buleon and V. Tran, *J. Mol. Biol.*, 1988, **201**, 365–378.
30 A. Imberty and S. Perez, *Biopolymers*, 1988, **27**, 1205–1221.
31 S. M. Lai, C. K. Huang and H. F. Shen, *J. Appl. Polym. Sci.*, 2005, **97**, 257–264.
32 H. Liu, F. Xie, L. Yu, L. Chen and L. Li, *Prog. Polym. Sci.*, 2009, **34**, 1348–1368.

